Synthesis of Ultra Small Biocompatible Magnetic Nanocomposites by Seeded Emulsion Polymerization

H. Kloust[*], E. Pöselt[*], S. Kappen[**], C. Schmidtke[*], A. Kornowski[*], W. Pauer[**], H.-U. Moritz[**], H. Weller[*]

[*]Institute of Physical Chemistry, University of Hamburg, Grindelallee 117, 20146 Hamburg, Germany, horst.weller@chemie.uni-hamburg.de
[**]Institute of Technical and Macromolecular Chemistry, University of Hamburg, Bundesstraße 45, 20146 Hamburg, Germany

ABSTRACT

We report an approach of seeded emulsion polymerization in which inorganic nanocrystals act as seeds. Ultrasmall biocompatible magnetic polymer coated nanocrystal could be prepared with sizes between 15 nm and 110 nm in a process that avoids any treatment with high shear forces or ultrasonication. The number of nanocrystals per seed and the shell thickness can be independently adjusted. Thus single encapsulated nanocrystals as well as clusters of nanocrystals can be obtained with thin or thick polymer shell. Polysorbat-80 was used as surfactant. It consists of poly(ethylene glycol) (PEG) chains, giving the particles outstanding biofunctional characteristics such as a minimization of unspecific interactions.

Keywords: seeded emulsion polymerization, nanocrystal, polysorbate-80, phase transfer, MRI

1 INTRODUCTION

Nanocrystals are high potentials in medical application, especially superparamagnetic ones, which are ideal contrast agents for magnetic resonance imaging (MRI). The phase transfer of the nanocrystals, that are hydrophobic after synthesis, into aqueous media is a challenge. An approach that allows the in-situ synthesis of polymer-stabilized nanocrystals in water is emulsion polymerization [1-8]. From the technical chemistry point of view these processes are highly favorable. To produce submicron composite latex particles, mini-emulsion polymerizations are frequently applied [9–13]. Hereby, the nanocrystals are dissolved in a monomer or a hydrophobic solvent and the emulsion is formed from the oil phase, kinetically driven by high shear rates or ultrasonification. For nanocrystal-polymer beads, typical diameters larger than 100 nm are obtained [1,14], however for most biological applications sizes of < 50 nm are required and controllable adjustment of the sizes are of special interest.

We present the production of PEGylated particles in the lower nanometer range by seeded emulsion polymerization technique under micro-emulsion conditions, avoiding any treatment with high shear forces or ultrasonication. Hereby, the hydrophobic shells of the inorganic nanocrystals are used as seeds for the seeded emulsion polymerization. As surfactant polysorbate-80, that contains poly(ethylene glycol) (PEG), was applied. PEG is known for its attribute to minimize unspecific interactions [15]. Furthermore polysorbate-80 has extraordinary properties in bioapplications and is used for drug delivery systems [16-18].

2 RESULTS AND DISCUSSION

Our apporach consists of two steps. The first step is the formation of the seed, where a tetrahydrofurane (THF) solution containing nanocrystals and polysorbate-80 (Scheme 1, A) is injected into water (Scheme 1, 1). The

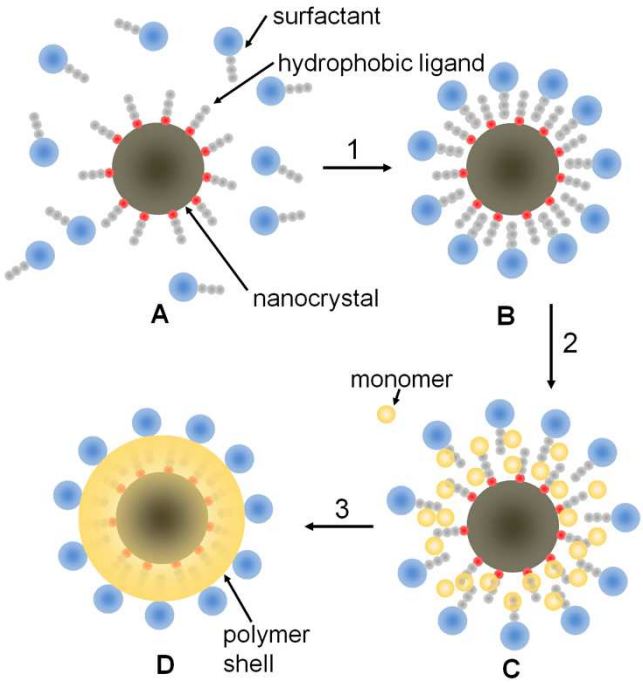

Scheme 1: Schematic illustration of encapsulation by seeded emulsion polymerization; A: nanocrystals and polysorbate-80 in THF; 1: injection into water; B: seed structure; 2: addition of monomer; C: swollen seed; 3: seeded emulsion polymerization; D: nanocrystal covered with a polymeric shell.

seed can consist of only one nanocrystal or can be a cluster of nanocrystals. The cluster size (aggregation number) can be tuned by the ratio between the nanocrystals and the polysorbate-80.

In the second step the monomer, styrene and divinylbenzene, is added to the solution (Scheme 1, 2) and the radical polymerization is started. This leads to a formation of a polymer shell around the nanocrystals. The thickness of the polymer shell can be tuned over a broad range by varying the amount of monomer added (Figure 1, (a)).

Transmission electron micrographs (TEM) of the final composites (Figure 1) show that the nanocrystals are surrounded by a polystyrene shell. In Figure 1 (c) and (d) single encapsulated iron oxide nanocrystals are presented. The thicker polymer shell of the composites in Figure 1 (c) results in a 35 nm higher hydrodynamic diameter compared to the composites shown in Figure 1 (d). In Figure 1 (e) and (f) shows differed sized clusters. Again, a proper coating of the nanocrystals by the polymer was found and the tuneability of the polymer shell in the case of clusters a seed could be demonstrated.

Atomic force microscopic (AFM) measurements of the composites showed, that the composites do not flatten on the substrate. Thus a stiff character of the polymer shell is indicated.

The colloidal solutions and the particle sizes were found to be stable over a period longer than six months at room temperature in water and for longer than 4 days in different biochemically relevant media. No significant changes in size were observed in Dulbecco's Phosphate-Buffered Saline (DPBS) with or without bovine serum albumin (BSA), 2-(N-morpholino)ethanesulfonic acid (MES), and sodium chloride (NaCl). Slight changes were observed in Dulbecco's Modified Eagle's Medium (DMEM) containing media (DMEM and fetal calf serum (FCS) as well as DMEM and 4-(2-hydroxyethyl)-1-piperazineethanesulfonic acid (HEPES)). Further more the composites were found to be stable in the pH-range of pH 3 to pH 12 and in the presence of small magnetic field gradient.

The magnetic properties of the composites are most relevant for MRI They depend on the saturation magnetization of the individual nanocrystals and the number of nanocrystal in a cluster. The transverse relaxivity r_2 increases, as shown in Figure 2, with increasing number of nanocrystal per composite, thus increasing hydrodynamic cluster diameter. r_2 was found to be between 50 $mM^{-1}s^{-1}$ and 330 $mM^{-1}s^{-1}$. For these experiments nanocrystals with a diameter of 11 nm were used. The use of smaller nanocrystals for example would result in a lower overall relaxivity. With increasing thickness of the polymer shell r_2 remains constant for small clusters and decreases slightly for larger clusters. This might be due to the increased interparticle distances arising from possible swelling. Detailed information on the influence of interparticle spacing within a cluster of nanocrystals have been reported recently [19].

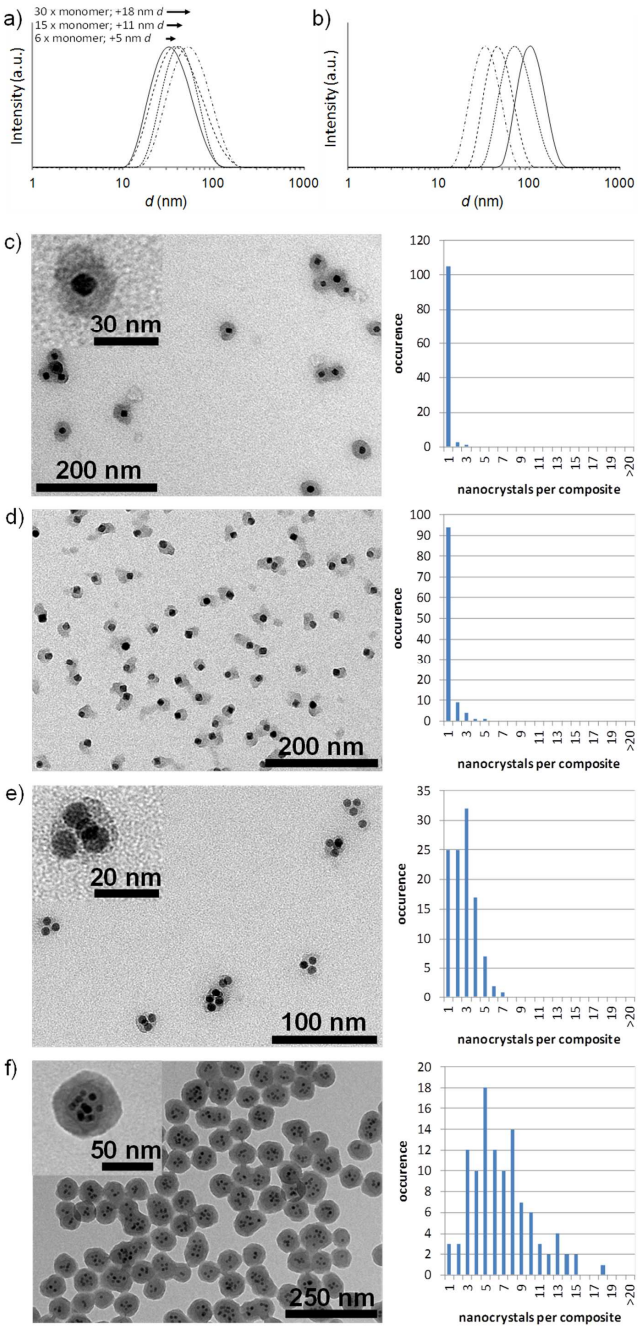

Figure 1: a): Dynamic light scattering (DLS) data (intensity distribution) showing the size tuneability of the polymer shell that increases from the continuous to the dashed and dotted up to the dot-dashed line, b): corresponding DLS data (intensity distribution) to the micrographs (– – = (c); – • – = (d); — — = (e); — = (f)), c) & d): TEM micrographs and corresponding histograms (109 composites each) of single encapsulated iron oxide-nanocrystals, e) & f) TEM micrographs and corresponding histograms (109 composites each) of clustered iron oxide-nanocrystals.

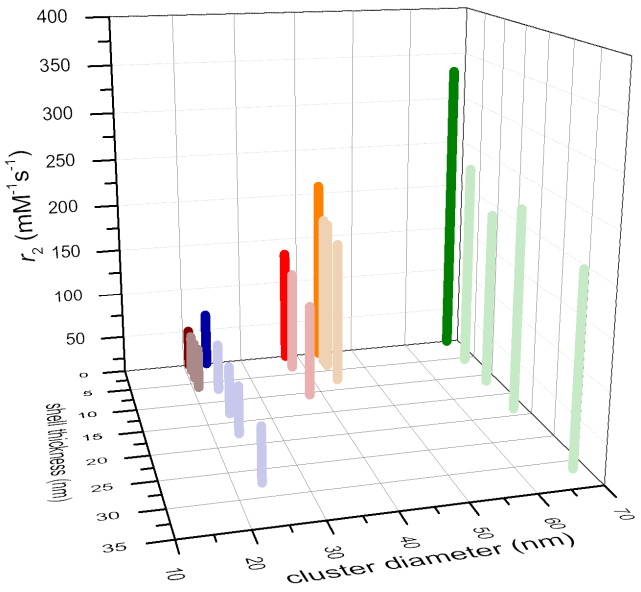

Figure 2: Effect of hydrodynamic cluster diameter (intensity distribution) and shell thickness on r_2, measured at 37 °C and 1.41 T. The semitransparent bars show the data after polymer shell growth.

With the described procedure hybrid structures can easily be produced. Different types of nanocrystals can be encapsulated in one latex sphere.

The ratio between the different kinds of nanocrystals can be tuned by the ratio of the nanocrystals added into the THF slution. As an example, Figure 3 shows Au-nanocrystals (4 nm) co-encapsulated with iron oxide-nanocrystals (9 nm). This enables the magnetic properties of the iron oxide-nanocrystals to be combined with the optical properties of the Au-nanocrystals. Figure 3 (a) shows scanning transmission electron micrographs (STEM) of the composites. Due to the higher z- contrast the Au-nanocrystals appear in these micrographs brighter than the iron oxide-nanocrystals. In addition Figure 3 (c) shows EDX element mapping of the composite. Iron oxide and gold nanocrystals are clearly to be distinguished. Oxygen appears as expected in the areas where iron is present. The absorption spectrum of these composites (Figure 3, (b)) shows the specific plasmon peak from the Au-nanocrystals.

3 CONCLUSION

In conclusion, seeded emulsion polymerization was used to encapsulate nanocrystals into using polysorbate-80 as surfactant, thus making them stable in water and biochemical relevant media under conservation of their characteristic properties. Polysorbate-80 was applied as the surfactant due to its extraordinary properties in bioapplications. To achieve highly uniform products, the formation was split into two simple steps, first the formation of the seed and second seeded emulsion

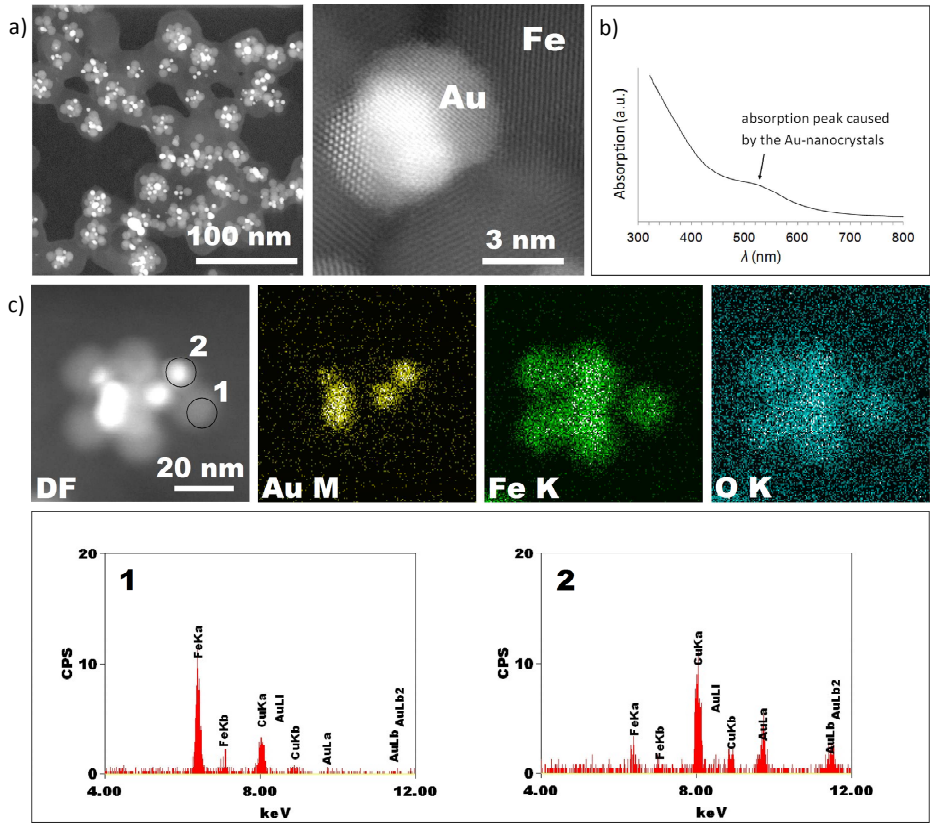

Figure 4: a): STEM overview (left) and HR-STEM micrograph (right) showing composite particles containing Au- and iron oxide-nanocrystals, b): the corresponding absorption spectrum clearly shows the gold plasmon band, c) upper part: from left to right: Dark field image, and EDX mapping at Au-M, Fe-K, O-K edge, lower part: EXD spectra of the selected areas in the dark field image.

NSTI-Nanotech 2012, www.nsti.org, ISBN 978-1-4665-6276-9 Vol. 3, 2012

polymerization. The number of nanocrystals per seed and the shell thickness can be independently adjusted. The high quality of the products could be documented in DLS, TEM and AFM as well as by optical examinations. The use of biocompatible substances, water as the reaction medium and low reaction temperatures of only 45 °C renders this approach to green syntheses. Finally, this approach allows the encapsulation of different kinds of hydrophobic nanocrystals. Thus it enables composite particles with different properties to be afforded.

ACKNOWLEDGMENT

We thank M. Ijeh for providing the gold nanocrystals, N. Reim for performing the AFM measurements and B. Freund for determination of iron concentration. We also thank CAN GmbH for providing nanocrystals and technical support. This work was supported by the European Union's Seventh Framework Programme (VIBRANT, FP7-228933-2) and the state excellence initiative “Nanotechnology in Medicine”.

REFERENCES

[1] K. Landfester, Angew. Chem., Int. Ed., 48, 4488–4507. 2009.
[2] K. J. Wormuth, Colloid Interface Sci., 241, 366–377, 2001.
[3] S. Yang, H. Liu, Z. J. Zhang, Polym. Sci., Part A: Polym. Chem., 46, 3900–3910, 2008.
[4] S. Fujii, D. P. Randall, S. P. Armes, Langmuir, 20, 11329–11335, 2004.
[5] A. Schmid, J. Tonnar, S. P. Armes, Adv. Mater., 20, 3331–3336, 2008.
[6] S. A. F. Bon, P. J. Colver, Langmuir, 23, 8316–8322, 2007.
[7] P. J. Colver, C. A. L. Colard, S. A. F. Bon, J. Am. Chem. Soc., 130, 16850–16851, 2008.
[8] J. Faucheu, C. Gauthier, L. Chazeau, J.-Y. Cavaille, V. Mellon, E. B. Lami, Polymer, 51, 6–17, 2010.
[9] K. Landfester, L. P. Ramirez, J. Phys.: Condens. Matter, 15, S1345–S1361, 2003.
[10] M. Zhang, G. Gao, C.-Q. Li, F.-Q. Liu, Langmuir, 20, 1420–1424, 2004.
[11] M. Peres, L. C. Costa, A. Neves, M. J. Soares, T. Monteiro, A. C. Esteves, A. Barros-Timmons, T. Trindade, A. Kholkin, E. Alves, Nanotechnology, 16, 1969–1973, 2005.
[12] K. Y. Berkel, A. M. van Piekarski, P. H. Kierstead, E. D. Pressly, P. C. Ray, C. J. Hawker, Macromolecules, 42, 1425–1427, 2009.
[13] C. Paquet, L. Page, A. Kell, B. Simard, Langmuir, 26, 5388–5396, 2010.
[14] N. Nabih, K. Landfester, A. Taden, J Polym Sci A: Polym Chem, 49, 5019–5029, 2011.
[15] P. Kingshott, H. J. Griesser, Curr. Opin. Solid State Mater. Sci., 4, 403–412, 1999.
[16] S. Wohlfart, C. Bernreuther, A. S. Khalansky, A. Theisen, J. Weissenberger, S. Gelperina, M. Glatzel, J. Kreuter, J. Nanoneurosci., 1, 144–151, 2009.
[17] S. E. Gelperina, A. S. Khalansky, I. N. Skidan, Z. S. Smirnova, A. I. Bobruskin, S. E. Severin, B. Turowski, F. E. Zanella, J. Kreuter, Toxicol. Lett., 126, 131–141, 2002.
[18] K. B. Kurakhmaeva, T. A. Voronina, I. G. Kapica, J. Kreuter, L. N. Nerobkova, S. B. Seredenin, V. Y. Balabanian, R. N. Alyautdin, Bull. Exp. Biol. Med., 145, 259–262, 2008.
[19] E. Pöselt, H. Kloust, U. Tromsdorf, M. Janschel, C. Hahn, C. Maßlo, H. Weller, ACS Nano, 6, 1619–1624, 2012.